

Supporting Information for

Fluorescent microspheres for one-photon and two-photon imaging of mesenchymal stem cells

Qi Zhang^{a,‡}, Jihua Nie^{a,‡}, Hong Xu^b, Yuyou Qiu^b, Xiaoran Li^{*c}, Wei Gu^a, Guangyu Tang^b, Judong Luo^{*d}

^a School of Radiation Medicine and Protection and School for Radiological and Interdisciplinary Sciences (RAD-X), Collaborative Innovation Center of Radiation Medicine of Jiangsu Higher Education Institutions, Medical College of Soochow University, Suzhou, Jiangsu 215123, China.

^b Department of Radiology, Shanghai Tenth People's Hospital, Tongji University School of Medicine, Shanghai 200072, China

^c Key Laboratory for Nano-Bio Interface Research, Division of Nanobiomedicine, Suzhou Institute of Nano-Tech and Nano-Bionics, Chinese Academy of Sciences, Suzhou, Jiangsu 215123, China

^d Department of Oncology, The Affiliated Changzhou No.2 People's Hospital With Nanjing Medical University, Changzhou, Jiangsu 213100, China

‡ Authors contributed equally.

Correspondence to:

*Email: xrli2010@sinano.ac.cn, Tel.: +86-(512) 6588-3941

*Email : judongluo@163.com

1. Preparation of PS fluorescent microspheres

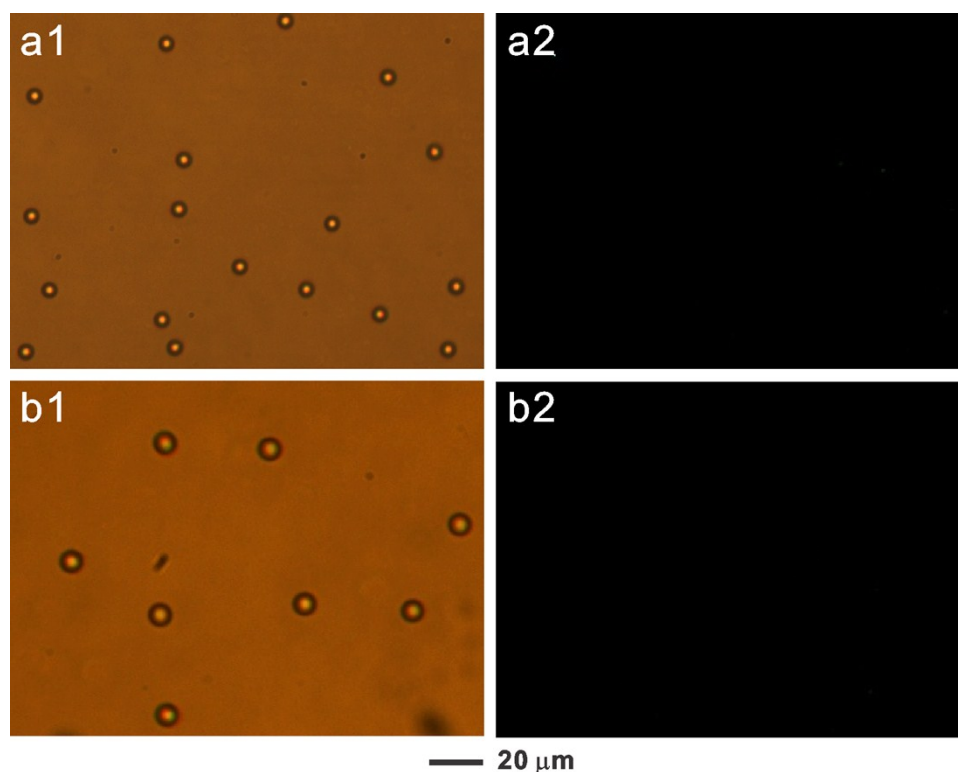


Figure S1. Micrographs of blank PS microspheres with diameter of 5.61 μm (a) and 9.94 μm (b). (a1,b1) bright field images, (a2,b2) excitation light of 559/34 nm with bandpass filter of 630/70 nm.

The digital micrographs (Figure S1) of blank PS microspheres illustrate the polymer beads exhibited good sphericity and well visible light transmittance. No autofluorescence signal was visible. Figure S2 shows the beads was stained with dyes using different chloroform content. It was found that the fluorescent signals can be clearly observed, and the intensity of fluorescent signals was increased with increasing of chloroform content. In the meanwhile, the number of doublet beads (aggregations) was also increased with an increase of chloroform content. The cross-linked PS beads can be swollen by the chloroform, and the released free polymer chains caused the beads linked with each other and consequently formed doublet

beads. In addition, the dye molecules may also contribute to the bead aggregation by enhancement of π - π stacking between beads and aromatic dye molecules.¹

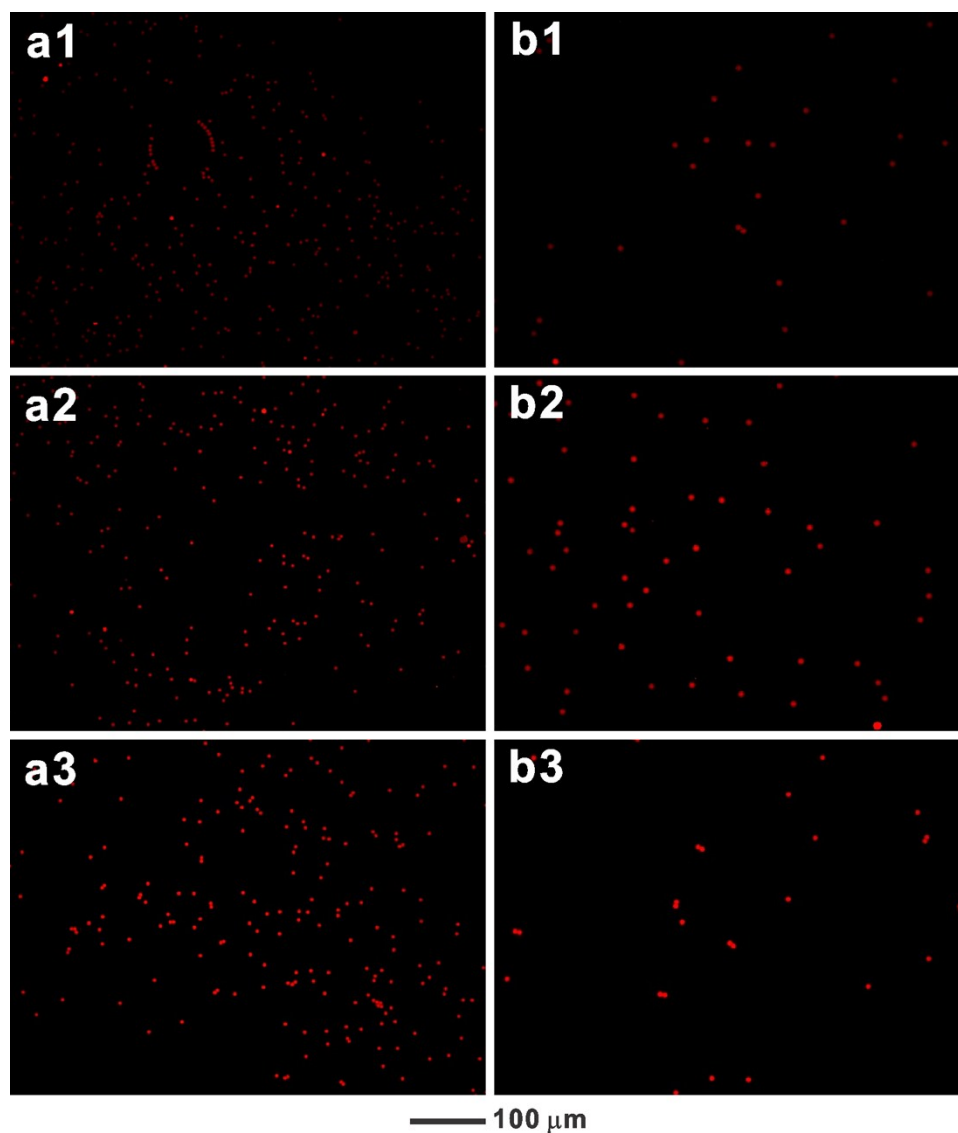


Figure S2. Fluorescence images of 5.61- μ m PS microspheres (a) and 9.94- μ m PS microspheres (b), captured with λ_{ex} of 559/34 nm and λ_{em} of 630/70 nm. The microspheres was stained in the mixture of isopropanol and chloroform containing 0 v/v % (a1,b1), 25 v/v % (a2,b2) and 50 v/v % (a3,b3) of chloroform, corresponding to the microspheres in Figure 2 of main manuscript.

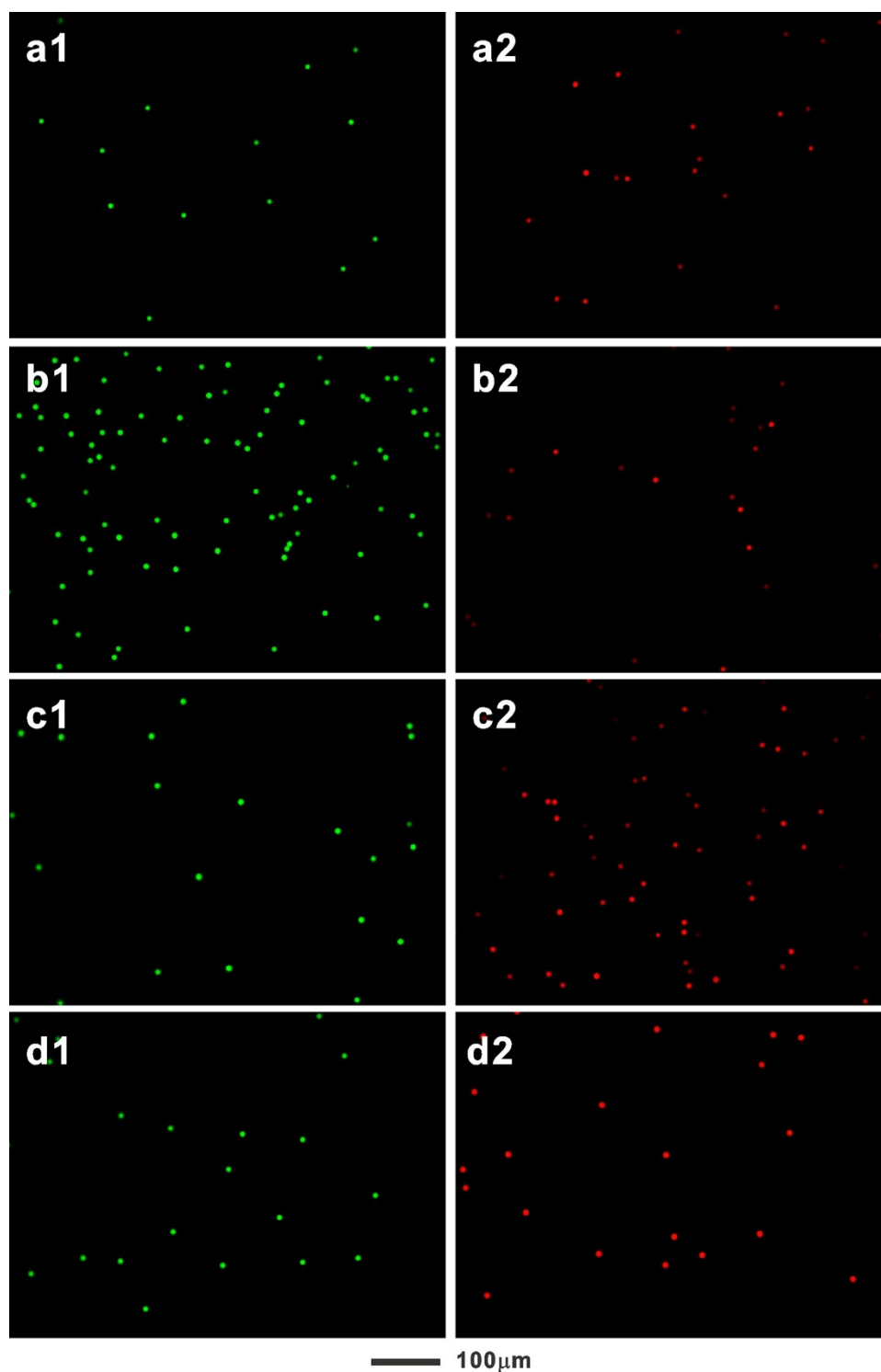


Figure S3. Fluorescence microscopy images of 5.61- μm PS microspheres stained with 1 mg AO and 1 mg RhB (a1,b1), 1 mg AO and 2 mg RhB (b1,b2), 2 mg AO and 2 mg RhB (c1,c2), and 2 mg AO and 4 mg RhB (d1,d2). (a1-d1), λ_{ex} 475/35 nm, λ_{em} 530/43 nm; (a2-d2), λ_{ex} 559/34 nm and λ_{em} 630/70 nm.

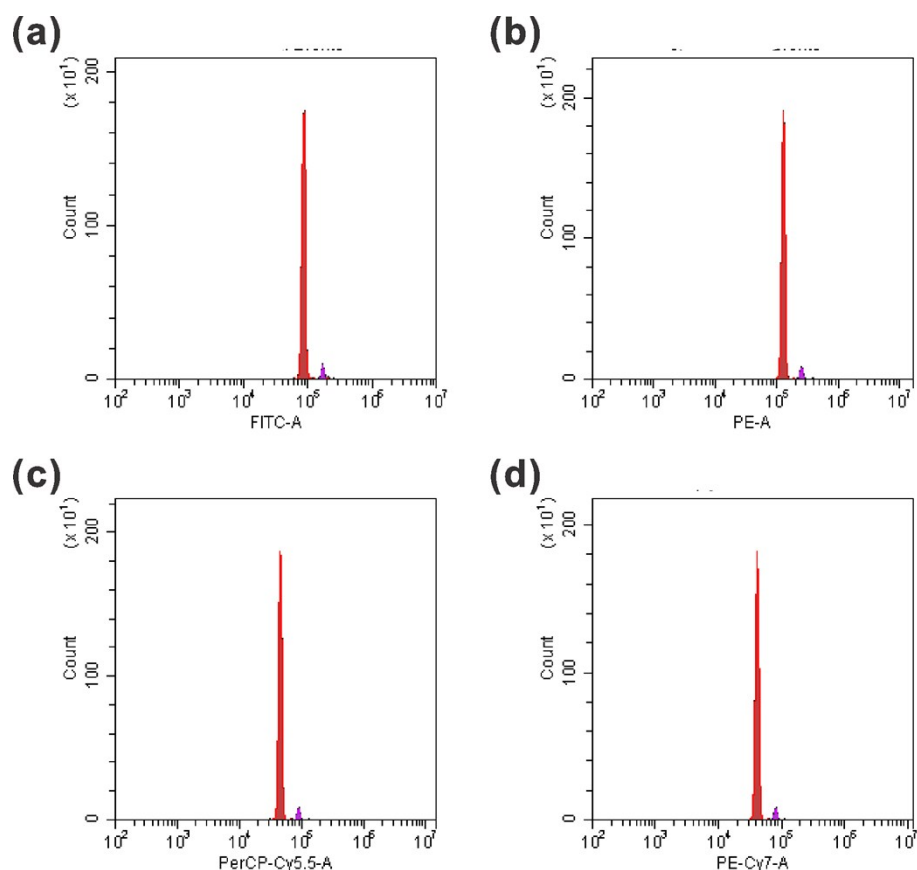


Figure S4. Flow cytometry analysis of 5.61- μm PS microspheres stained with 2 mg AO and 4 mg RhB. The signals in FITC, PE, PerCP-Cy5.5 and PE-Cy7 channels were recorded using bandpass 530/30 nm (a), 585/40 nm (b), 700/75 nm (c) and 780/40 nm (d) filters, respectively.

The influence of AO and RhB concentration on bead fluorescence intensity was investigated. The stained beads were analyzed using fluorescent microscopy and flow cytometry. As illustrated in Figure S3, both green and red colors can be visualized for the broad emission spectrum. The bead intensity was gradually augmented with increasing of AO and RhB concentrations. When 2 mg AO and 4 mg RhB was used, a bright and uniform fluorescence was observed. Moreover, very strong signals in FITC, PE, PerCP-Cy5.5 and PE-Cy7 channels (Figure S4) can be detected simultaneously, due to the efficient energy transfer from AO to R101 at λ_{ex} of 488

nm.^{2,3} Since the signals in PE-Cy7 channel were quite high, it's safe to predict the fluorescent PS beads can be used as control agents in diverse applications.

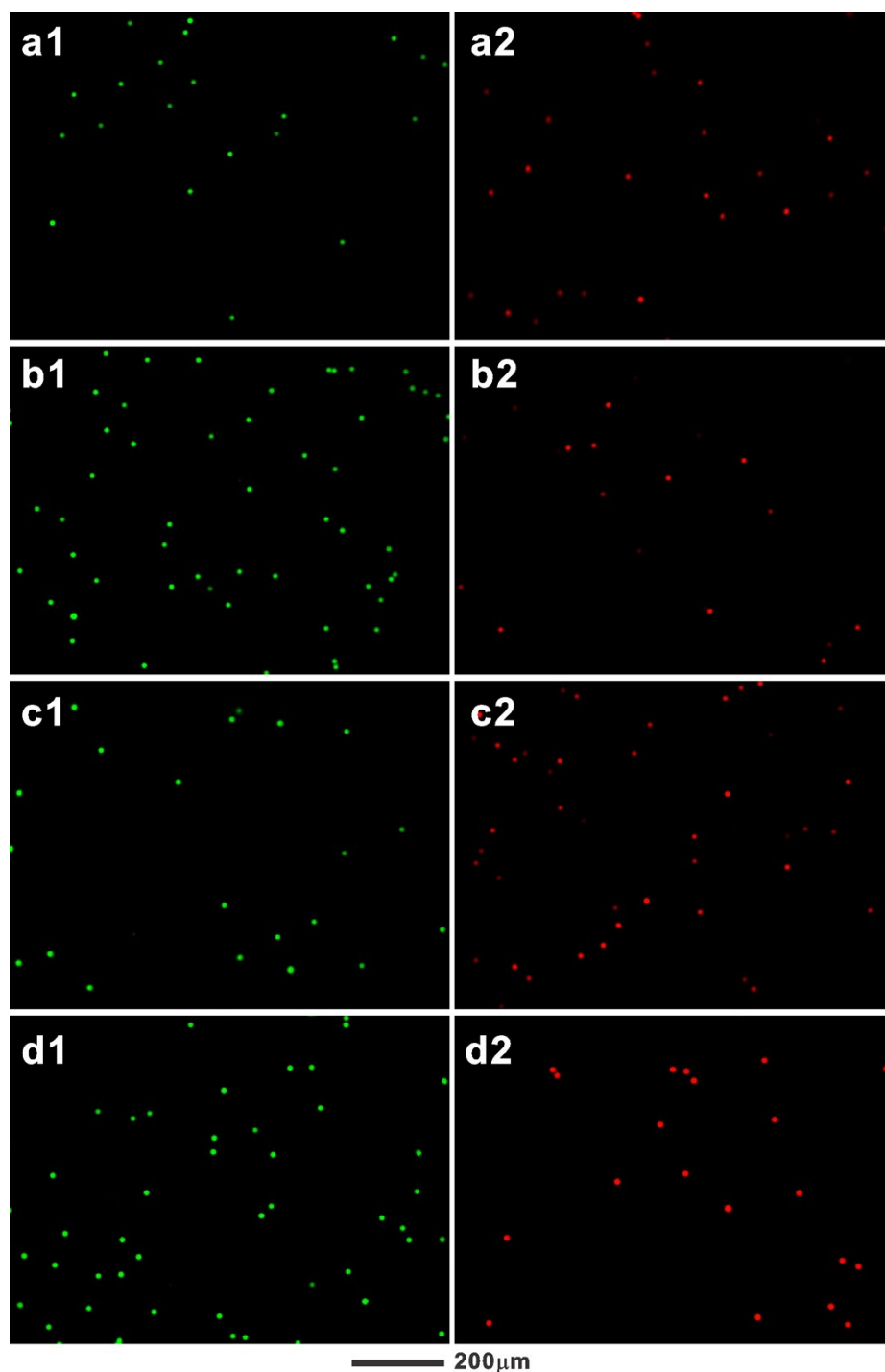


Figure S5. Fluorescence microscopy images of 9.94- μm PS microspheres prepared with 1 mg AO and 1 mg RhB (a1,b1), 1 mg AO and 2 mg RhB (b1,b2), 2 mg AO and 2 mg RhB (c1,c2), and 2 mg AO and 4 mg RhB (d1,d2). (a1-d1), λ_{ex} 475/35 nm, λ_{em} 530/43 nm; (a2-d2), λ_{ex} 559/34 nm and λ_{em} 630/70 nm.

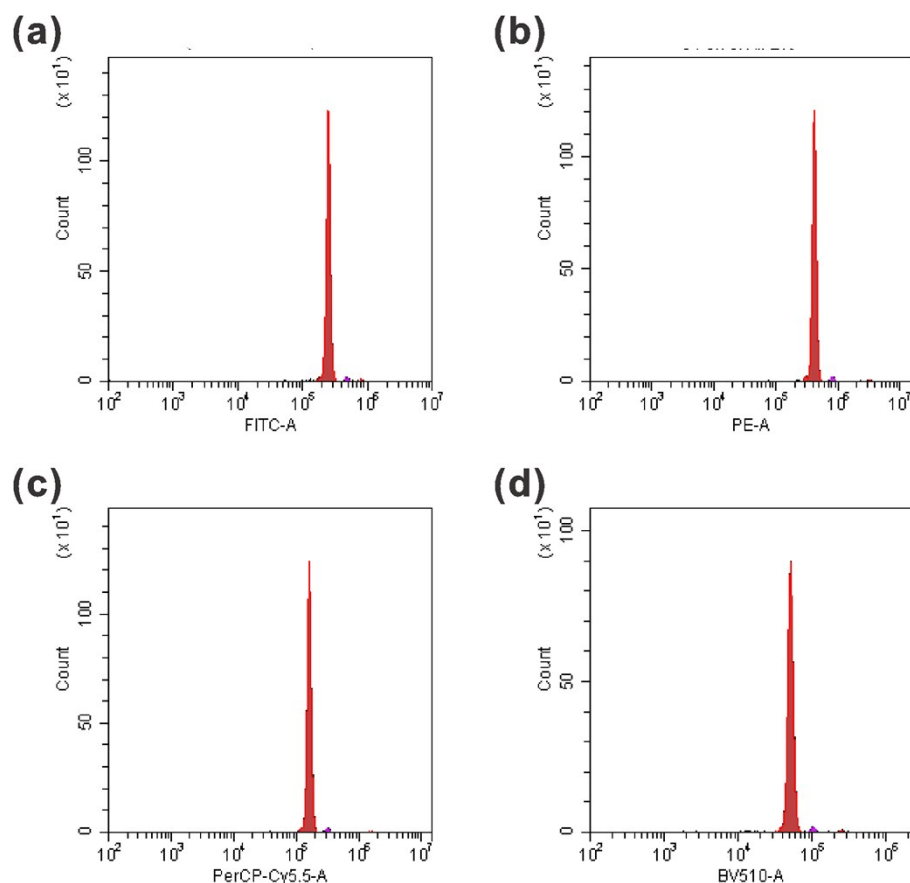


Figure S6. Flow cytometry analysis of 9.94- μm PS microspheres synthesized with 2 mg AO and 4 mg RhB. The signals in FITC, PE, PerCP-Cy5.5 and PE-Cy7 channels were recorded using bandpass 530/30 nm (a), 585/40 nm (b), 700/75 nm (c) and 780/40 nm (d) filters, respectively.

Similarly, 2 mg AO and 4 mg RhB was the optimal concentration for the staining of 9.94- μm PS microspheres. For 9.94- μm beads (Figure S5 and S6), the average intensities of fluorescent signals in FITC, PE, PerCP-Cy5.5 and PE-Cy7 channels were around 2-3 times of those of 5.61- μm beads. Considering that the volume of 9.94- μm beads was 5.5 times of 5.61- μm bead volume, the 9.94- μm beads were hard to be brightly stained in the same experimental conditions as compared with 5.61- μm bead.

2. Photostability of fluorescent microspheres

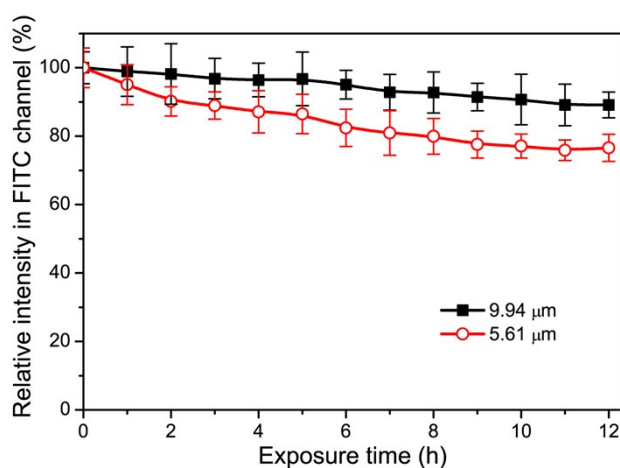


Figure S7. Temporal evolution of fluorescence decay of 9.94- μm and 5.61- μm PS microspheres irradiated by UV light (365 nm, 100 W). The fluorescent signals in FITC channel were recorded by using Flow cytometer equipped with a bandpass 530/30 nm filter.

The photostability of fluorescent microspheres plays an important role in their usage, storage and lifetime. The 9.94- μm and 5.61- μm PS microspheres were irradiated under rigorous UV condition to evaluate their photostability by means of Flow cytometry.⁴ Figure S7 plots temporal evolution of fluorescent signal decay of PS beads in FITC channel. It was found that the fluorescent intensities of PS beads were both gradually decreased. After 12 h irradiation, the signal intensities of 9.94- μm and 5.61- μm PS beads decreased to 89.1% and 76.6% of initial values, respectively. The result demonstrated that both the 9.94- μm and the 5.61- μm fluorescent microspheres possessed remarkable photostability, which can meet the stability requirement of biomedical imaging. In addition, the 9.94- μm fluorescent microspheres exhibited a better photostability compared with 5.61- μm beads, which might be ascribed to the higher light shield effect of thicker polymer matrix.

3. Cytotoxicity of AO-PLGA nanospheres and fluorescent microspheres

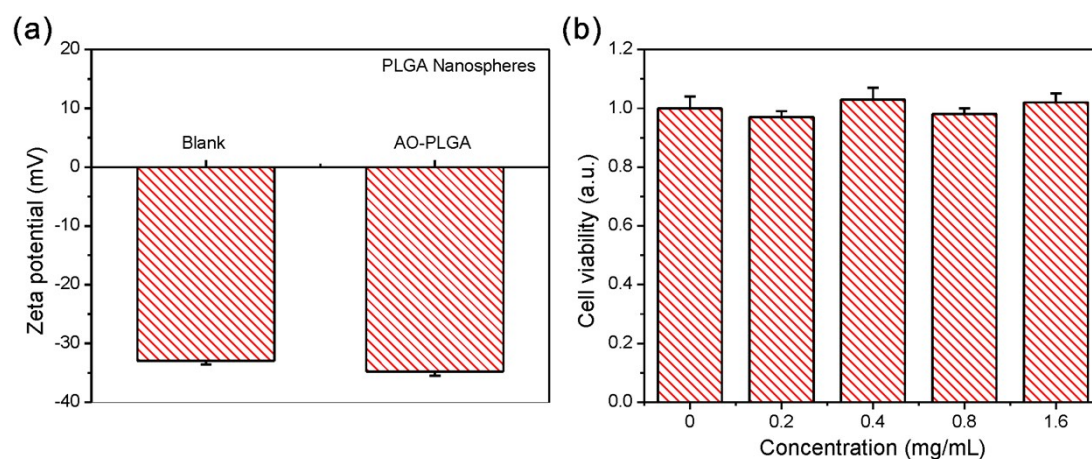


Figure S8. (a) The Zeta potential values of blank PLGA and AO-PLGA nanospheres.

(b) Cell viability of hMSCs incubated with AO-PLGA nanospheres for 48 h.

The cell viability assay was evaluated by using of the colorimetric 3-(4,5-dimethylthiazol-2-yl)-2,5-diphenyltetrazolium bromide (MTT, CCK8, Dojindo) test. In Brief, following hMSCs incubation with AO-PLGA nanospheres for 48 h, the media were aspirated and replaced with 100 μ L of serum-free media. Each well was added 10 μ L of an MTT stock solution (5 mg/mL), followed by incubation for 4 h at 37 $^{\circ}$ C. The supernatant was removed, and cells were lysed with 100 μ L DMSO.⁵ As shown in Figure S8b, the cell viability after the treatment with nanospheres did not change much, compared to the untreated control. Even at the concentration of 1.6 mg/mL nanospheres, there was almost no change in cell viability. The results indicated low cytotoxicity of AO-PLGA nanospheres. PEG and PLGA have been approved for clinical use by the Food and Drug Administration (FDA) of the US.^{6,7} Therefore, the AO-PLGA nanospheres, prepared with the most widely used co-polymers, were demonstrated to be biocompatible in the experiment of stem cells imaging.

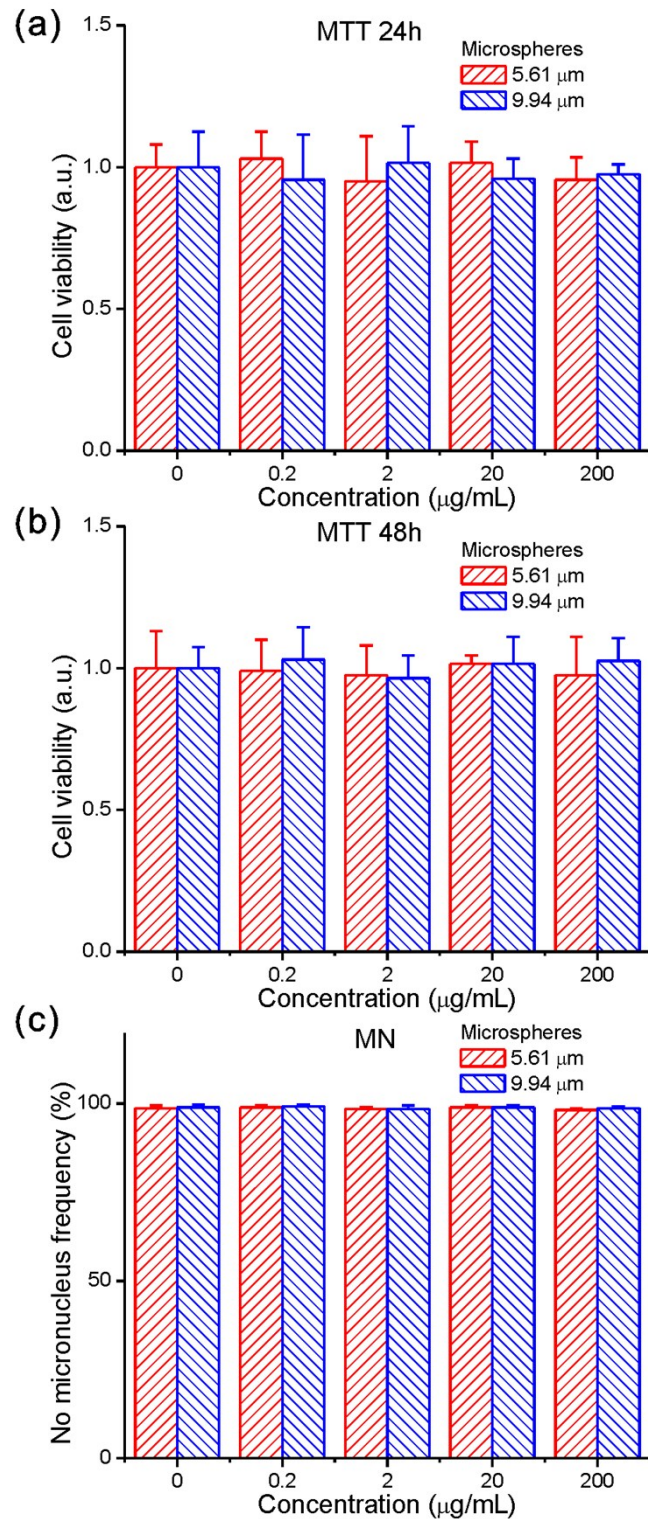


Figure S9. Cell viability (a,b) and micronucleus frequency (c) of HBE cell incubated with 5.61- μm and 9.94- μm fluorescent microspheres. The cytotoxicity was assessed using MTT assay at 24 h (a) and 48 h (b), and micronucleus test at 24 h (c).

MTT assay and micronucleus test of fluorescent microspheres

HBE cell line was maintained in DMEM containing 10% FBS, L-glutamine (2 mM), non-essential amino acids (2 mM), penicillin (100 U/mL), and streptomycin (100 U/mL) (Gibco, Grand Island, NY, USA) at 37 °C under 5% CO₂ atmosphere.

MTT assay was applied to evaluate cytotoxicity effect of 5.61- μ m and 9.94- μ m fluorescent microspheres on proliferation and viability of HBE cells. MTT salt is cleaved by mitochondrial dehydrogenase in the metabolic active cells and is reduced to an insoluble formazan crystal which displays a purple color. The color was detected by a microplate reader. HBE cells at log-phase were seeded into 96-well plate at 5×10^3 density and randomly divided into 0, 0.2, 20 and 200 μ g/mL groups. After 24 h or 48h incubation, the supernatant was removed. 20 μ L sterile MTT was added into each test well in triplicates for 4 h, then the supernatant was completely removed, with the addition of 150 μ L dimethyl sulfoxide for 10 min vortex until the complete resolving of crystal violet. Absorbance values were measured at 570 nm in a microplate reader. The proliferation rate was calculated in each group. All MTT experiments were repeated a minimum of three times.

Micronucleus test was used to detect the potential genotoxic compounds. Cells were randomly divided into 0, 0.2, 20 and 200 μ g/mL groups as treated above for 24 hours. 10^4 cells in each group were gently spread onto multiple clean microscope slides and allowed to dry. The slides were stained for 5 min in filtered 4 v/v% Giemsa in Gurr's phosphate buffer, pH 6.8, rinsed, dried, and mounted with coverslips. Cytotoxicity was measured using microscope. Coded slides were analyzed by scoring 1000 binucleate cells from each culture for micronuclei.

The MTT test results of 5.61- μ m and 9.94- μ m microspheres at 24 h and 48 h showed in Figure S9a and S9b, respectively. It was demonstrated that there were no differences compared to control groups in cell viability.

The micronucleus results were illustrated in Figure S9c. It was indicated that there was no significant change in different groups.

References

1. M. Cao, A. Fu, Z. Wang, J. Liu, N. Kong, X. Zong, H. Liu and J. J. Gooding, *J. Phys. Chem. C*, 2014, **118**, 2650-2659.

2. D. Yu, G. Zou, X. Cui, Z. Mao, I. Estrela-Lopis, E. Donath and C. Gao, *J. Mater. Chem. B*, 2015, **3**, 8865-8873.
3. L. Liu, X. Fei, S. Zhu, L. Yu and B. Zhang, *Langmuir*, 2013, **29**, 5132-5137.
4. Y. Zhong, F. Peng, F. Bao, S. Wang, X. Ji, L. Yang, Y. Su, S.-T. Lee and Y. He, *J. Am. Chem. Soc.*, 2013, **135**, 8350-8356.
5. Y. Zhang, S. F. Ali, E. Dervishi, Y. Xu, Z. Li, D. Casciano and A. S. Biris, *ACS Nano*, 2010, **4**, 3181-3186.
6. S. H. Ranganath, Y. Fu, D. Y. Arifin, I. Kee, L. Zheng, H.-S. Lee, P. K. H. Chow and C.-H. Wang, *Biomaterials*, 2010, **31**, 5199-5207.
7. S. Chen and J. Singh, *Int. J. Pharm.*, 2008, **352**, 58-65.